A Hierarchically Porous Carbon Fabric for Highly Sensitive Electrochemical Sensors

Yuan Jiao, Seong Won Cho, Suyoun Lee, Sang Hoon Kim, Seung-Yeol Jeon, Kahyun Hur, Sun Mi Yoon, Myoung-Woon Moon,* and Aiying Wang*

The hierarchically porous carbon fabrics with controlled conductivity and hydrophilicity have been fabricated by dual templating method of soft templates nested on hard templates. A non-woven fabric coated with a solution of F127/resol has been carbonized for the synthesis of both macro-porous structures of 10–15 μm in diameter having meso-porous carbon structures of 4–6 nm, respectively. After carbonization treatment, not only conductivity is significantly improved, the hierarchically porous carbon also shows superhydrophilicity or water-absorbing nature due to mild hydrophilic material and its dual scale roughness. The porous carbon becomes conductive with resistivity widely tuned from 5.4×10^3 Ωm to 3.1×10^{-3} Ωm by controlling the carbonization temperature. As the increased wettability for organic liquids could lead organic molecules deep into carbonized fabrics, the sensitivity of hierarchically porous carbon fabrics benefits the detection for methanol(CH_3OH) or hydrogen peroxide (H_2O_2). This new design concept of hierarchically porous structures having the multi-functionality of high wettability and conductivity can be highly effective for electroanalytical sensors.

1. Introduction

Porous materials have received a great deal of attention since it poses the high specific surface area, diverse porous structure, stability in different chemical environments, and easy accessibility,[1] which can be used for gas adsorption or liquid separation,[2] catalysis,[3] electric,[4] and battery[5] fields. In addition to the porosity, the conductivity and hydrophilicity are major key factors for the case of electrochemical sensors or biosensors used in biochemical applications such as the detection of H_2O_2 or methanol.[6] H_2O_2 is an important reactive oxygen species generated in biochemical reactions,[7] and considered as one of the major risk factors of disease-related pathophysiological complications. Monitoring H_2O_2 levels, therefore, is particularly important. In other cases, low performance[8] and methanol crossover[9] are the two main obstacles in the fabrication of direct methanol fuel cells (DMFC), where the precise measurement of the methanol concentration is crucial. For both fields, porous conductive carbon has proven to be a highly stable and reproducible matrix for the fabrication of sensors.[10]

The high conductivity meets the demand for the electrochemical signal transduction,[11] while the open channels of hierarchical nanostructure, along with the continuously conductive framework, provide a relatively short diffusion path.[12,13] It was suggested that the hydrophilicity through surface modification can increase in sensitivity under liquid solution[14] due to better liquid-solid contact, which can be also achieved by the macroscale roughness. Ultimately, high hydrophilicity and sensing resolution can be achieved by macroscale and meso-scale porous structures, respectively.

Motivated by these promising properties, many efforts have been made to synthesize porous carbon materials,[15–17] of which dual templating combining soft and hard templates has become a promising method. Hierarchical porous materials synthesized by dual templating own high surface area, easy accessibility to active sites, and high mass transport and diffusion rate at the same time. The meso-pores can provide sufficient channels for ion diffusion to improve electrochemical performance while macro pores facilitate ion transport via shorter ion diffusion distance and lower resistance.[18] The fabrication techniques have been used with silica or organic materials as hard templates impregnating with appropriate carbon precursor, followed by carbonization of the composite and the removal of template,[19] resulting in the ordered macro- and meso-structure.[20–23] Besides high active sites, the introduction of meso-pores into a micro- or macro-porous structure

Dr. Y. Jiao, Prof. A. Wang
Key Laboratory of Marine Materials and Related Technologies, Zhejiang Key Laboratory of Marine Materials and Protective Technologies, Chinese Academy of Sciences, Ningbo Institute of Materials Technology and Engineering, Ningbo 315201, P. R. China
E-mail: aywang@nimte.ac.cn

Dr. M.-W. Moon, Dr. Y. Jiao, Dr. S. H. Kim, Dr. S.-Y. Jeon, Dr. K. Hur, Dr. S. M. Yoon
Materials and Life Science Research Division, Korea Institute of Science and Technology, Seoul 136-791, Republic of Korea
E-mail: mwmoon@kist.re.kr

Dr. Y. Jiao
University of Chinese Academy of Sciences, Beijing 100049, P. R. China

Dr. S. W. Cho, Dr. S. Lee
Electronic Materials Research Center, Korean Institute of Science and Technology, Seoul 136-791, Republic of Korea

**ADVANCED
SCIENCE NEWS**

www.advancedsciencenews.com

**ADVANCED
ENGINEERING
MATERIALS**

www.aem-journal.com

provides size and shape selectivity for reactants, intermediates, and products, thus hierarchically porous products have been widely used as catalysts[24,25] or catalyst supports,[26] separation process,[27] energy conversion,[28] and storage.[18,29–31] However, unlike porous structures made of materials like metal,[32,33] polymer,[34] or silica,[35] the superhydrophilic property has been less utilized on the hierarchical porous carbon materials with conductive nature to improve the sensibility for electrochemical molecules.

In this paper, hierarchically porous carbon fabrics were developed by adding two main functions of the hydrophilicity and controlled conductivity through a dual-templating approach, which used Pluronic F127 as the soft template and non-woven fabrics as the hard template. The macro-porous structures from polymeric fabrics and the meso-porous structures from block polymers were successfully emulated by forming hierarchical carbon structures in different scales. After carbonization treatment, not only conductivity has been significantly improved, the hierarchically porous carbon showed super-hydrophilicity or water-absorbing nature due to mild hydrophilic material and its roughness. It was found that a carbonized PET (polyethylene terephthalate) with hierarchically porous structure (HC-PET for short) sheet allows water penetrate easily deep inside. The resistivity of HC-PET was tuned widely by varying the carbonization temperature, which was applied for the sensors detecting methanol and H_2O_2 solutions with various concentrations. Combining the superhydrophilicity and widely tuned conductivity, HC-PET is suggested as a promising material used as a liquid detector for electroanalytical biosensors.

2. Results and Discussion

2.1. Morphology and Microstructure

The comparison between PET and HC-PET sheet is demonstrated in **Figure 1**a. The SEM images of the pristine PET fabric revealed a random 3D interconnecting network with macro-pores of several tens of micrometers (Figure 1b). When the pristine PET sheet was immersed into the F127/resol solution, the mixture adhered to the PET fibers, forming a thin film. After carbonization, this film became a meso-porous carbon skeleton of the HC-PET sheet. During the carbonization process, the PET fibers decomposed, then became cylindrical pores of a few tens of micrometers in diameter. There were some parts of the PET fibers which were not covered by F127/resol, which became channel-like passages as seen in Figure 1b and c. These passages enhanced the capillarity and helped water penetrate into the inside of HC-PET sheet, thus the hydrophobic PET fabric became superhydrophilic HC-PET sheet. On the other hand, as a soft template, the decomposition of F127 led to the formation of a meso-porous structure as discussed with Figure 1e and f.

As rectangular pieces of non-woven PET (inset of Figure 1b) were used as hard template, both the C-PET and HC-PET fabrics kept their rectangular shape with a very small amount of shrinkage in length (inset of Figure 1d). It could also be observed that the resol between fibers was connected and formed a film when the fibers were close enough to each other. Since the

phenolic resol adhered to the surface of the PET fibers, the decomposition of PET during carbonization, led to the formation of cylindrical pores with diameter of 10–15 μm, while the phenolic resol became a porous network skeleton. The difference between HC-PET and C-PET was attributed to the existence of meso-pores originated from the decomposition of F127. On even larger magnification of HC-PET, it is revealed that ordered meso-structures formed over a large domain. SEM (Figure 1e) acted as indirect evidence for the presence of meso-porous structure here. The walls of meso-pores were presented as ups while pores as downs, showing bump-like structures in its contrast. The TEM images further confirmed the pore structures. As displayed in Figure 1f, the HC-PET showed uniform cylindrical meso-pores with pore size around 4–6 nm which was formed by the decomposition of F127. Since the meso-porous structure was nested on the macro-prous structure, this structure was defined as a hierarchical porous structure, thus the carbonized PET with hierarchical porous structure defined as HC-PET. Furthermore, the surface topologies of C-PET and HC-PET were compared by using AFM. The surface topology of C-PET in Figure 1g shows the smooth roughness with no periodic patterns in meso-scale. However, the line profile of HC-PET in Figure 1h indicates the periodic patterns of bumps or holes in around 13.3–22.5 nm, which is close to the peak-to-peak distance of 11.6 nm (Figure 1f), proving the existence of periodic meso-pores on macro-porous fabric structures.

The soft template F127 owns a high oxygen content and exhibits a low thermal stability as compared to phenolic resol, which has a 3D network structure resulting from polymerization. As the F127 was decomposed during pyrolysis, it resulted in meso-porous materials with pore sizes ranging from 2[36] to 32 nm.[37] The pore distribution and specific surface area of the HC-PET were investigated from the nitrogen sorption isotherms, as shown in **Figure 2**a. The N_2 adsorption–desorption isotherm of the HC-PET was a type-IV curve, according to IUPAC classification,[38] with an H_2-type hysteresis loop, similar to previously reported meso-porous materials,[36] indicating uniform cylindrical pores. The pore size distributions derived from the adsorption branches by using the BJH model[39] indicated a pore size of 3.4 nm, and a BET surface area of $407 \, m^2 \, g^{-1}$.

Surface chemical composition and morphology are the two key factors affecting the surface functions. FT-IR was used to compare the functional groups' changes between PET, C-PET, and HC-PET. As shown in Figure 2b, in the PET fabric, the ester carbonyl bond stretching led to the peak at $1717 \, cm^{-1}$, vibration at $1470–1350 \, cm^{-1}$ resulted from the ethylene glycol segment, and the ester group stretching led to $1247 \, cm^{-1}$ peak. However, all of these polar functional groups were decomposed during pyrolysis, as proven by the disappearance of these FT-IR vibration bands in both C-PET and HC-PET FT-IR spectra.

2.2. Wetting Properties of HC-PET

In electrochemical systems such as DMFCs, the crossover happens through the active transport of the protons and water, or diffusion through either the water-filled pores or the electrolyte
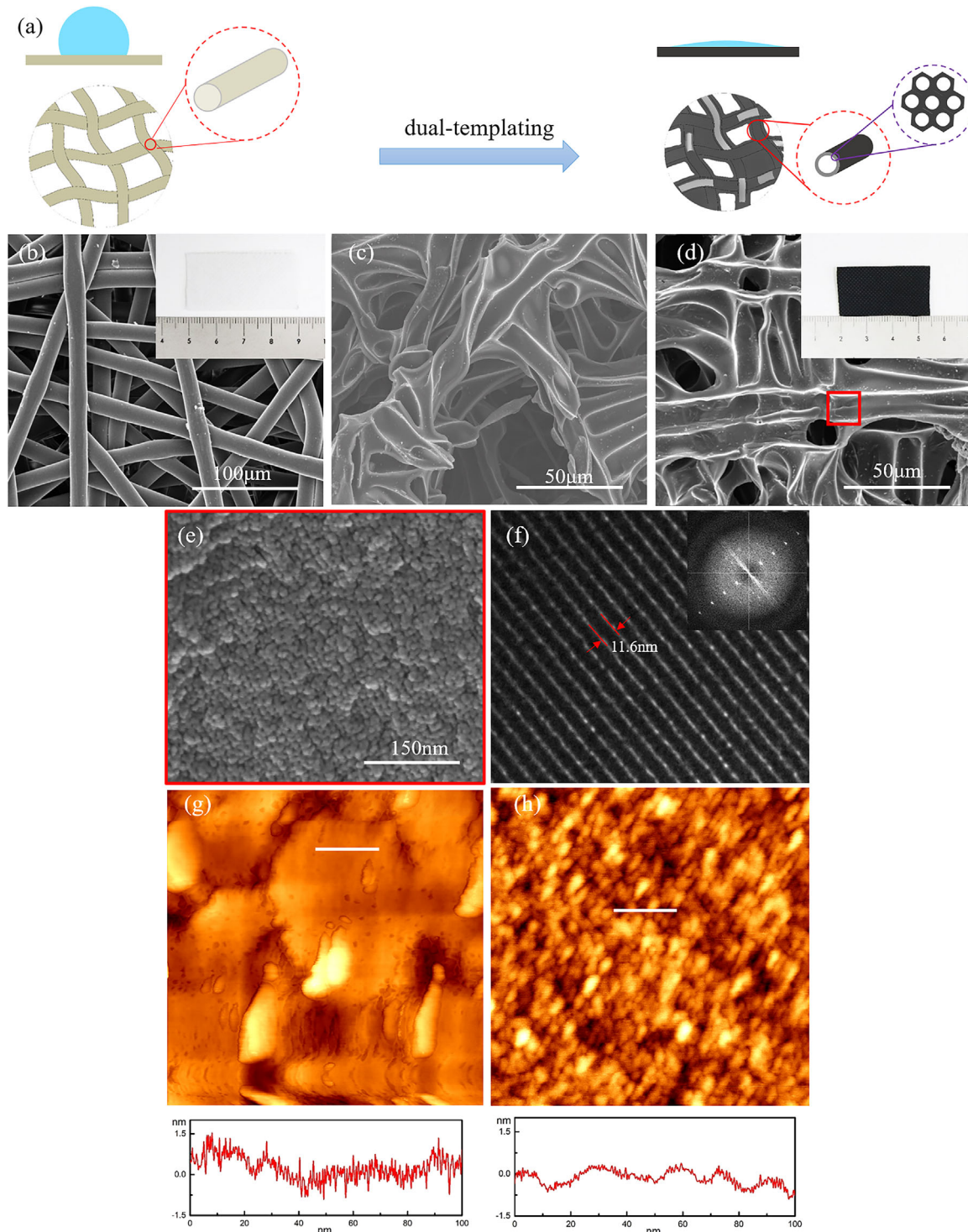
Figure 1. a) Scheme for comparison in structure between pristine PET and HC-PET fabrics; SEM images of b) pristine PET, c) C-PET sheet and d) HC-PET; e) locally magnified HC-PET fiber over a large domain; f) TEM and the corresponding fast Fourier transform (FFT) image; AFM profiles of g) C-PET, and h) HC-PET.

membrane itself.[40] H_2O_2-related cell activities take place in cells with water as the main component. Since both situations are in aqueous conditions, the hydrophilicity is one of the most important surface properties, and in particular, better

hydrophilicity would favor better contact between the surface and solution in liquid conditions.

Figure 3 shows the characterized CAs for the water and H_2O_2 solution. For the pristine PET surface, as shown in Figure 3a, the
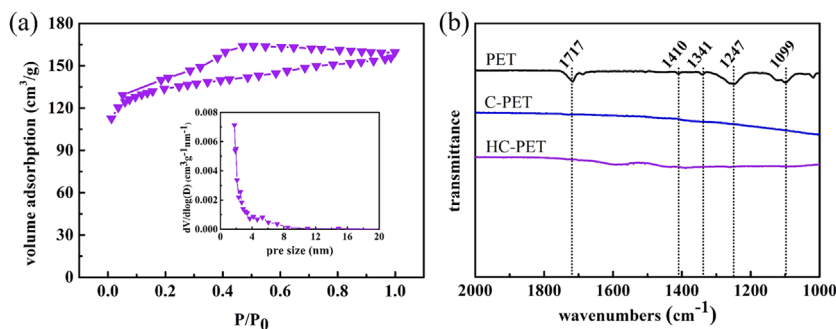
Figure 2. a) N$_2$ adsorption–desorption isotherms of the HC-PET sheet; b) FT-IR data of PET, C-PET, and HC-PET fabrics.
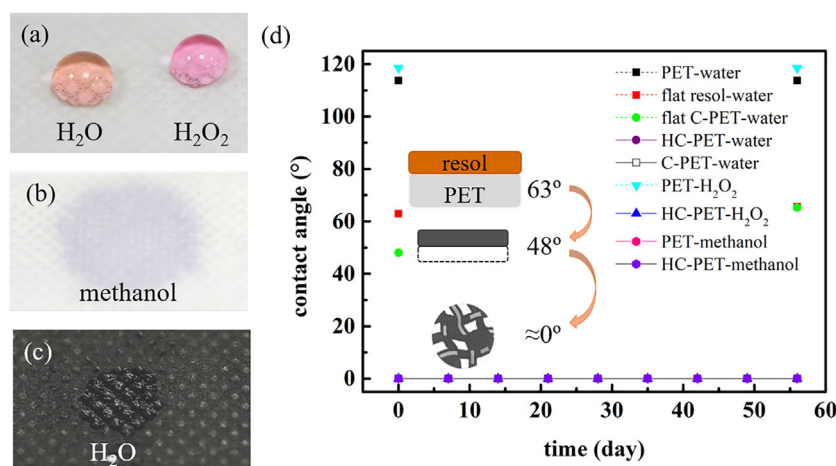
Figure 3. a) Water and H$_2$O$_2$ liquid drops and b) methanol on the pristine PET; c) spread water drop on HC-PET; d) the CAs of different liquids on various samples in ambient condition.
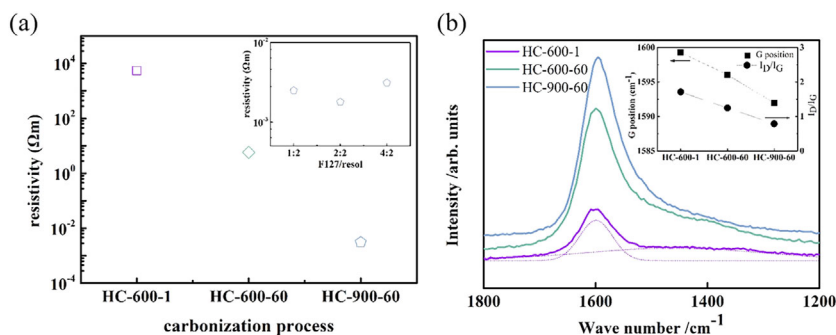
Figure 4. a) Resistivity of HC-PETs produced by different carbonization process, insert showed resistivity of HC-900-60 samples with different F127/resol ratios; b) Raman spectra of HC-PETs produced by different carbonization process, insert showed G peak position and I$_D$/I$_G$ information.

CA for the DI water (surface tension $\approx$72.8 mN m^{-1}) and H$_2$O$_2$ (74 mN m^{-1}) solution showed 113.7° and 118.5°, respectively, while the methanol spread quickly over the surfaces because of the lower surface tension of 22.70 mN m^{-1} (Figure 3b). For the

C-PET and HC-PET, however, all of the liquids showed a superwetting behavior having CAs of near zero. When a drop of water or H$_2$O$_2$ was on HC-PET, it spread and quickly permeated through the macro-porous structure, as illustrated in Figure 3c.

To check the effect of macro-pores or meso-pore on wettability, a flat resol film without any porous structure, a porous material with only meso-pores (flat C-PET), and a porous material with only macro-pores (C-PET) were also prepared. The water CA for the flat resol was 63°, which showed the mild hydrophilicity of the porous material. Since the meso-pores in flat C-PET increased the surface area by comparison to the flat resol, the water CA decreased to 48° (Figure 3d). As for the C-PET and HC-PET fabrics, due to the mild hydrophilicity of the material nature and wicking phenomenon through macro-porous structure, the apparent water CAs became near zero. Figure 3d shows the change in wettability for three liquids. The interesting result was that the apparent CAs of three liquids on the HC-PETs could last for around 60 days, if it was kept under ambient atmosphere.

2.3. Liquid Detection Ability of HC-PET

The resistivity of the HC-PET sheet in different methanol solutions was measured using the "Van der Pauw" method.[41] The conductivity of HC-PET can be adjusted by changing the carbonization conditions.[42] Conventionally, the carbonization process is usually carried out at 900 °C for 60 min (HC-900-60 in short), ensuring the carbonized product maintains good conductivity. HC-900-60 samples with various F127/resol ratios all showed good conductivity with resistivity lower than 3.50×10^{-3} Ωm in air (**Figure 4**a, an insert). This evidence agreed well with the hypothesis, in which the conductivity of the HC-PET was not sensitive to the templates. However, if the carbonization process was carried out under lower temperatures, 600 °C for example, the conductivity decreased significantly shown in Figure 4. Specifically, the resistivity of the HC-PET carbonized at 600 °C for 1 min (HC-600-1) increased up to 5.43×10^3 Ωm. Raman spectra were analyzed for assessing the crystallinity of carbonized samples which affected the conductivity majorly changed with the sp^2 clustering in carbon matrix and the ratio of the intensity in the disordered graphite sp^2 (denoted as the D peak) to the ordered graphite-like sp^2 bonded carbon (denoted as the G peak). As shown in Figure 4b, all samples showed amorphous carbon
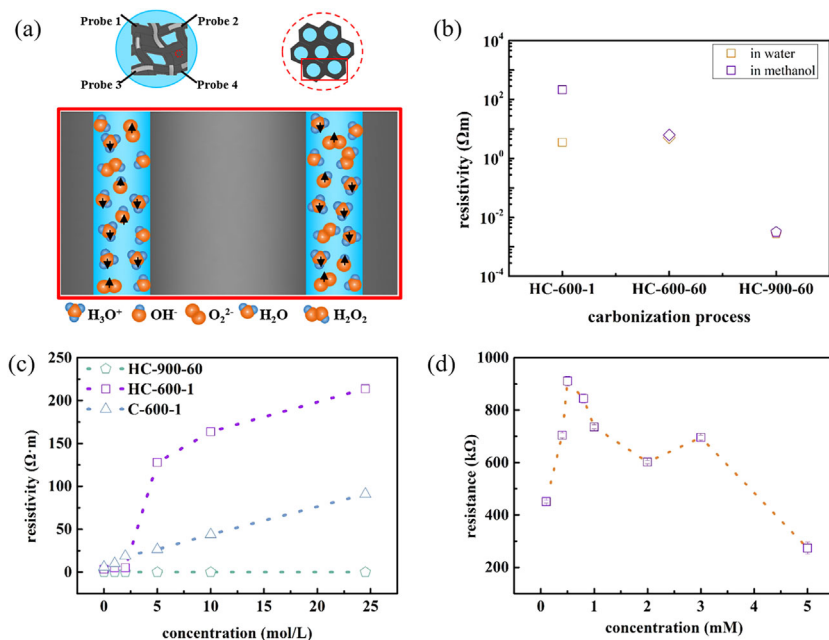
Figure 5. a) The scheme for liquid concentration detection; b) HC-PET sheets produced from different carbonization processes for water or methanol; c) resistivity changes of different porous materials in methanol solutions with different concentration; d) resistivity changes of HC-600-1 in H_2O_2 solutions with different concentration.

spectra which consisted D peak and G peak. With increasing carbonization temperature or duration (an insert in Figure 4b), G peak position was lower due to higher sp^2 clustering[43] which would increase the conductivity in amorphous carbon materials.[44] On the other hand, the ratio of the intensity of D peak and G peak (I_D/I_G) also suggested changes in sp^2 clusters. The decrease in I_D/I_G was resulted from the conversion of disordered sp^2 clusters to ordered sp^2 microcrystals, increasing the crystalline thickness,[45] thus increased conductivity of HC-PETs.

Liquid concentration was detected using the "Van der Pauw" method, as seen in **Figure 5**a. When the HC-PET was immersed into the solution, its pores filled with liquid, thus increasing the contact area between the HC-PET surface and electrolytes. Furthermore, we found that the conductivity of the HC-PET was strongly dependent on the liquid conditions used. The electrical conductivity of water was higher than that of methanol,[46] due to the self-ionization in water. As a result, when HC-PET was immersed into water or methanol, the changes in current could be detected sensitively.

The HC-PET sheets were produced under different carbonization processes, all showing the variation in conductivity

between water and methanol. However, differences existed in the way the charge carriers moved.[47] HC-900-60 had the best conductivity, with the charge carriers flowing mainly through the carbon skeleton, while the HC-600-1 displayed the worst conductivity, so that the ions not only flowed through the carbon skeleton but also through the liquid. This difference benefited HC-600-1 much better sensitivity than HC-900-60 in concentration detection. As shown in Figure 5b, the resistivity of the HC-900-60 sheet was $2.86 \times 10^{-3}\,\Omega m$ in DI water, and $3.26 \times 10^{-3}\,\Omega m$ in 99.97 wt% methanol. There was almost no change in the resistivity while immersed into solutions with different concentrations. Conversely, the poor conductive HC-600-1 showed a resistivity change from $3.50\,\Omega m$ in DI water to $2.14 \times 10^2\,\Omega m$ in 99.97 wt% methanol. Methanol concentration has been reported to have a nearly linear relation with solution conductivity, which varied around 78% when methanol concentration increased by 1 M.[48] Taking advantage of this behavior, the concentration of methanol solution was detected using HC-600-1. As shown in Figure 5c, the resistivity changed approximately 24 times when the methanol concentration was increased, from $5.04\,\Omega m$ in 2 M to $1.27 \times 10^2\,\Omega m$ in 5 M solution. Such a change in resistivity proved the high resolution of HC-PET as a promising methanol concentration detector. C-PET carbonized at 600 °C for 1 min (C-600-1 in short) owning only macro-porous structure was also compared to the result for HC-600-1. When methanol concentration increased from 2 to 5 M, it showed relative slight changes in resistivity from 18.80 to 26.45 Ωm, which was much less than that of HC-600-1. It has been reported that the higher surface area in meso-scale is, the better sensitivity obtained for methanol detection.[49,50] Therefore, the mesoporous structure of HC-600-1 resulted in the higher surface area for ion adsorption than C-600-1 without meso-scale structure,[51] which ultimately led to the higher sensitivity in methanol concentration detection for HC-600-1.

Similar to the detection of methanol, monitoring the concentration of H_2O_2 is also of great importance due to its vital role in biological modifications, including modern medicine and environmental control.[7,52] Consequently, the selective and quantitative detection of H_2O_2 is another crucial investigation for our fabricated porous carbon materials. Figure 5d shows

Table 1. The samples and their responsive treatment condition.

Sample	Hard template	Soft template	F127/resol ratio	Carbonization temperature [°C]	Carbonization duration [min]
HC-PET	PET fabric	F127	0.5/2,1/2 or 2/2	600	1
C-PET	PET fabric	none	0/2	600	1
flat C-PET	PET film	F127	1/2	600	1
flat resol	PET film	None	0/2	600	1

**ADVANCED
SCIENCE NEWS**

www.advancedsciencenews.com

**ADVANCED
ENGINEERING
MATERIALS**

www.aem-journal.com

Table 2. HC-PET with F127/resol = 1/2 under different carbonization conditions.

Sample	Hard template	Soft template	F127/resol ratio	Carbonization temperature [°C]	Carbonization duration [min]
HC-600-1	PET fabric	F127	1/2	600	1
HC-600-60	PET fabric	F127	1/2	600	60
HC-900-60	PET fabric	F127	1/2	900	60

the different responses of HC-600-1 in H_2O_2 solutions with different concentrations. The change in resistance could reach as high as 900% when the concentration was varied by only 1 mM. As stated in previous work,[11] non-activated porous carbon with a resistance of 25 Ωm had a sensitivity to H_2O_2 of 11.40 μA mM^{-1}. Compared with the reported work, the fabricated HC-600-1 materials with hierarchical structure as well as the facile synthesis advantages make it very promising for C-PET application in wide liquid concentration detections.

3. Conclusion

Hierarchically porous carbon materials through the combination of soft and hard templating were introduced with special functions of conductivity and superhydrophilicity. Phenolic resol acted as a carbon precursor, while block polymer was used for the soft template, and non-woven PET fabrics served as the hard template, forming meso-pores and macro-pores with carbonization process, respectively. the wettability was further enhanced to superhydrophilicity by the roughness in pores on macro-porous structure and mild hydrophilicity of C-PET and HC-PET sheets, so that water could spread and penetrate inside macro-structures. During the pyrolysis process, the carbonization degree was controlled so as to create HC-PET with the proper conductivity used for electrochemical sensors for the detection of methanol and H_2O_2 concentration. Hierarchical porous HC-PET owned higher surface area in meso-scale for higher ion adsorption sites favored to get better sensitivity than C-PET without meso-pores structure. The HC-PET fabric demonstrated a large responsive change in resistivity when liquid concentration varied, which makes it a promising material as a liquid concentration detector for high-efficiency biochemical sensors and electroanalytical measurements.

4. Experimental Section

Materials: PET fabrics were purchased from a local market. They were cleaned with ethanol and deionized (DI) water then dried under a 50 °C in an oven. All chemicals, including phenol (≥ 99%, redistilled), formaldehyde solution (37 wt% in H_2O), NaOH, HCl (hydrochloric acid), tetrahydrofuran (THF), chloroform ($CHCl_3$), and Pluronic F127 (H(OC_2H_4)$_x$(OC_3H_6)$_y$(OC_2H_4)$_z$OH) were purchased from Sigma–Aldrich (Yongin, Republic of Korea).

Sample Preparation: As reported previously, phenol-formaldehyde resol was synthesized using phenol and formaldehyde solution with NaOH as a catalyst.[36] Typically, 6.1 g of phenol was melted in a three-neck flask at 40–42 °C. 1.3 g of 20 wt% NaOH aqueous solution was stirred in. After 10 min, 10.5 g of formalin solution was carefully added dropwise over 10 min. The slightly orange-colored solution was further heated to 70–75 °C. After stirring for 1 h, the solution was cooled to room

temperature, neutralized using 0.6 mol l^{-1} (M) of HCl solution, then freeze-dried overnight. The resol was then dissolved in a mixture of THF and $CHCl_3$ (1:1, *w:w*). The resulting cloudy solution was filtered through a PTFE (polytetrafluoroethylene) syringe filter (0.45 μm) to remove the precipitated sodium chloride, dried again using a rotation evaporator, and dissolved in ethanol as a 20 wt% solution. The HC-PET was synthesized as PET sheets immersed into F127/phenolic resol ethanol solution, followed by heat treatment. In a typical preparation, 0.5 g of F127 was dissolved in 10.0 g of ethanol. Then, 5.0 g of 20 wt% resol solution containing 1 g resol was added. After stirring for 10 min, a homogeneous solution was obtained. A piece of PET film was used instead of PET fabric sheets to get a flat carbonized PET (flat C-PET for short). For different ratios of F127/resol, 0.25 and 1 g of F127 was mixed with 5.0 g of 20 wt% resol solution for F127/resol = 0.5/2 and 2/2, respectively. F127/resol = 0/2 was used for the fabrication of macro-porous carbonized PET fabric (C-PET for short) samples without meso-porous structure due to no soft templating material (**Table 1**). The solution was poured into a dish, and 3 g of PET sheets were immersed in the solution for 5 h, before the lid was removed to let the ethanol evaporate for an additional 2 h. Heat treatment was composed of two parts: thermal polymerization and pyrolysis. The thermal polymerization process was carried out under atmospheric conditions, in a 120 °C oven for 24 h and the pyrolysis process under Ar atmosphere with a flow rate of 100 sccm. The temperature was first increased to 350 °C for 3 h, and then increased to 600 °C for 1 min for the carbonization. To produce HC-PET with different conductivity, the carbonization process was set at 600 and 900 °C for 60 min with the heating rate of 1 °C min^{-1} (**Table 2**).

Characterization: The morphology of the HC-PET was observed with a scanning electron microscope (SEM, Nova, FEI) and a transmission electron microscope (TEM, TITAN, FEI). The topography images of C-PET and HC-PET were measured in 500 × 500 nm^2 with an atomic force microscope (AFM, Park systems Co., XE-70) in non-contact mode. The contact angle (CA) was measured through a sessile drop test. To measure the CA, 3 μl droplets of liquids, including DI water, H_2O_2, and methanol, were deposited on the solid surfaces using a microsyringe. The Brunauer–Emmett–Teller (BET) specific surface area was measured by N_2 adsorption isotherms using a pore size analyzer (ASAP 2020, Micromeritics, USA) at 77 K. The pore volumes and pore size distributions were derived using the Barrett–Joyner–Halenda (BJH) method. A Fourier transform infrared spectroscopy (FT-IR, NICOLET iS10, Thermo Fisher) was used to characterize the surface chemical properties. Raman spectra (In Via Raman Microscope, Renishaw) were characterized for three samples of HC-600-1, HC-600-60, and HC-900-60 using a 244 nm UV laser power and output power 100 mW. For liquid concentration detection, the HC-PET was cut into 5 mm × 5 mm pieces and the current–voltage (I–V) characteristic was measured using the "Van der Pauw" method. The electrical contacts to specimens were formed using silver epoxy (EPO-TEK H20E, Epoxy Technology) and gold wires. A Source-Measure unit (Keithley 2636) and an electrometer (Keithley 6517B) were used for low- and high-resistive specimens, respectively.

Conflict of Interest

There is no conflict of interest.

Keywords

porous carbon, dual-templating, multi-functional, sensor

[1] S. De, A. M. Balu, J. C. van der Waal, R. Luque, *Chem. Cat, Chem.* **2015**, *7*, 1608.

[2] J.-H. Oh, T.-J. Ko, M.-W. Moon, C. H. Park, *RSC Adv.* **2014**, *4*, 38966.

[3] X. Liu, Y. Zhou, W. Zhou, L. Li, S. Huang, S. Chen, *Nanoscale* **2015**, *7*, 6136.

[4] T. A. Silva, H. Zanin, P. W. May, E. J. Corat, O. Fatibello-Filho, *ACS Appl. Mater. Interfaces* **2014**, *6*, 21086.

[5] H. Li, F. Shen, W. Luo, J. Dai, X. Han, Y. Chen, Y. Yao, H. Zhu, K. Fu, E. Hitz, L. Hu, *ACS Appl. Mater. Interfaces* **2016**, *8*, 2204.

[6] A. Walcarius, *TrAC Trends Anal. Chem.* **2012**, *38*, 79.

[7] Y. Zhang, X. Bai, X. Wang, K. K. Shiu, Y. Zhu, H. Jiang, *Anal. Chem.* **2014**, *86*, 9459.

[8] A. Aricò, D. Sebastian, M. Schuster, B. Bauer, C. Urso, F. Lufrano, V. Baglio, *Membranes* **2015**, *5*, 793.

[9] S. Almheiri, H. Liu, *Int. J. Hydrogen Energy* **2015**, *40*, 10969.

[10] V. G. Gavalas, N. A. Chaniotakis, T. D. Gibson, *Biosens. Bioelectron.* **1998**, *13*, 1205.

[11] S. Sotiropoulou, V. Gavalas, V. Vamvakaki, N. Chaniotakis, *Biosens. Bioelectron.* **2003**, *18*, 211.

[12] L. Pan, G. Yu, D. Zhai, H. R. Lee, W. Zhao, N. Liu, H. Wang, B. C.-K. Tee, Y. Shi, Y. Cui, *Proc. Natl. Acad. Sci.* **2012**, *109*, 9287.

[13] D. Zhai, B. Liu, Y. Shi, L. Pan, Y. Wang, W. Li, R. Zhang, G. Yu, *ACS Nano.* **2013**, *7*, 3540.

[14] I. Taurino, S. Carrara, M. Giorcelli, A. Tagliaferro, G. De Micheli, *Sens. Actuators B* **2011**, *160*, 327.

[15] W. Dai, S. J. Kim, W.-K. Seong, S. H. Kim, K.-R. Lee, H.-Y. Kim, M.-W. Moon, *Sci. Rep.* **2013**, *3*, 2524.

[16] N. Bouts, A.-A. El Mel, B. Angleraud, P.-Y. Tessier, *Carbon* **2015**, *83*, 250.

[17] E. M. Susca, P. A. Beaucage, M. A. Hanson, U. Werner-Zwanziger, J. W. Zwanziger, L. A. Estroff, U. Wiesner, *Chem. Mater.* **2016**, *28*, 2131.

[18] D. W. Wang, F. Li, M. Liu, G. Q. Lu, H. M. Cheng, *Angew. Chem., Int. Ed.* **2008**, *47*, 373.

[19] S. Dutta, A. Bhaumik, K. C. W. Wu, *Energy Environ. Sci.* **2014**, *7*, 3574.

[20] Y. H. Deng, C. Liu, T. Yu, F. Liu, F. Q. Zhang, Y. Wan, L. J. Zhang, C. C. Wang, B. Tu, P. A. Webley, H. T. Wang, D. Y. Zhao, *Chem. Mater.* **2007**, *19*, 3271.

[21] C. Xue, J. Wang, B. Tu, D. Zhao, *Chem. Mater.* **2009**, *22*, 494.

[22] N. Brun, S. R. S. Prabaharan, C. Surcin, M. Morcrette, H. Deleuze, M. Birot, O. Babot, M.-F. Achard, R. Backov, *J. Phys. Chem. C* **2012**, *116*, 1408.

[23] Q. Li, R. Jiang, Y. Dou, Z. Wu, T. Huang, D. Feng, J. Yang, A. Yu, D. Zhao, *Carbon* **2011**, *49*, 1248.

[24] Q. M. Sun, N. Wang, D. Y. Xi, M. Yang, J. H. Yu, *Chem. Commun.* **2014**, *50*, 6502.

[25] J. Liu, G. Y. Jiang, Y. Liu, J. C. Di, Y. J. Wang, Z. Zhao, Q. Y. Sun, C. M. Xu, J. S. Gao, A. J. Duan, J. Liu, Y. C. Wei, Y. Zhao, L. Jiang, *Sci. Rep.* **2014**, *4*, 7276.

[26] Y. Wei, T. E. Parmentier, K. P. de Jong, J. Zecevic, *Chem. Soc. Rev.* **2015**, *44*, 7234.

[27] T. Y. Ma, H. Li, A. N. Tang, Z. Y. Yuan, *Small* **2011**, *7*, 1827.

[28] N. Jiang, X. Y. Yang, G. L. Ying, L. Shen, J. Liu, W. Geng, L. J. Dai, S. Y. Liu, J. Cao, G. Tian, T. L. Sun, S. P. Li, B. L. Su, *Chem. Sci.* **2015**, *6*, 486.

[29] C.-H. Huang, R.-a. Doong, D. Gu, D. Zhao, *Carbon* **2011**, *49*, 3055.

[30] J. Liang, X. Du, C. Gibson, X. W. Du, S. Z. Qiao, *Adv. Mater.* **2013**, *25*, 6226.

[31] Z. Wang, E. R. Kiesel, A. Stein, *J. Mater. Chem.* **2008**, *18*, 2194.

[32] Y.-Z. Chen, G. Cai, Y. Wang, Q. Xu, S.-H. Yu, H.-L. Jiang, *Green Chem.* **2016**, *18*, 1212.

[33] Y. Lin, Y. Shen, A. Liu, Y. Zhu, S. Liu, H. Jiang, *Mater. Des.* **2016**, *103*, 300.

[34] J. Yu, S. Han, J. S. Hong, O. Sanyal, I. Lee, *Langmuir* **2016**, *32*, 8494.

[35] Y. Li, Z. Zhang, B. Ge, X. Men, Q. Xue, *Green Chem.* **2016**, *18*, 5266.

[36] Y. Meng, D. Gu, F. Zhang, Y. Shi, L. Cheng, D. Feng, Z. Wu, Z. Chen, Y. Wan, A. Stein, *Chem. Mater.* **2006**, *18*, 4447.

[37] C. Liu, M. Yu, Y. Li, J. Li, J. Wang, C. Yu, L. Wang, *Nanoscale* **2015**, *7*, 11580.

[38] K. S. Sing, *Pure Appl. Chem.* **1985**, *57*, 603.

[39] E. P. Barrett, L. G. Joyner, P. P. Halenda, *J. Am. Chem. Soc.* **1951**, *73*, 373.

[40] T. Schultz, S. Zhou, K. Sundmacher, *Chem. Eng. Technol.* **2001**, *24*, 1223.

[41] A. Ramadan, R. Gould, A. Ashour, *Thin Solid Films* **1994**, *239*, 272.

[42] J. G. Werner, S. S. Johnson, V. Vijay, U. Wiesner, *Chem. Mater.* **2015**, *27*, 3349.

[43] C. Casiraghi, A. Ferrari, J. Robertson, *Phys. Rev. B* **2005**, *72*, 085401.

[44] J. Robertson, *Mater. Sci. Eng. R: Rep.* **2002**, *37*, 129.

[45] Y.-R. Rhim, D. Zhang, D. H. Fairbrother, K. A. Wepasnick, K. J. Livi, R. J. Bodnar, D. C. Nagle, *Carbon* **2010**, *48*, 1012.

[46] C. Edmondson, P. Stallworth, M. Wintersgill, J. Fontanella, Y. Dai, S. Greenbaum, *Electrochim. Acta* **1998**, *43*, 1295.

[47] B. Van Zeghbroeck, Principles of Semiconductor Devices, Colarado University, Boulder, USA **2004**, Chapter 1.

[48] M. L. Hainstock, Y. Tang, *Int. J. Anal. Chem.* **2015**, *2015*, 106173.

[49] E. Comini, G. Faglia, G. Sberveglieri, Y. Li, W. Wlodarski, M. Ghantasala, *Sens. Actuators B* **2000**, *64*, 169.

[50] G.-J. Li, X.-H. Zhang, S. Kawi, *Sens. Actuators B* **1999**, *60*, 64.

[51] Z. Peng, D. Zhang, L. Shi, T. Yan, S. Yuan, H. Li, R. Gao, J. Fang, *J. Phys. Chem. C* **2011**, *115*, 17068.

[52] A. A. Karyakin, E. A. Puganova, I. A. Budashov, I. N. Kurochkin, E. E. Karyakina, V. A. Levchenko, V. N. Matveyenko, S. D. Varfolomeyev, *Anal. Chem.* **2004**, *76*, 474.